

Reassessing the Human Immunodeficiency Virus Type 1 Life Cycle through Age-Structured Modeling: Life Span of Infected Cells, Viral Generation Time, and Basic Reproductive Number, R_0 ^{∇†}

Christian L. Althaus,* Anneke S. De Vos, and Rob J. De Boer

Theoretical Biology, Utrecht University, 3584 CH Utrecht, The Netherlands

Received 27 August 2008/Accepted 11 May 2009

The rapid decay of the viral load after drug treatment in patients infected with human immunodeficiency virus type 1 (HIV-1) has been shown to result from the rapid loss of infected cells due to their high turnover, with a generation time of around 1 to 2 days. Traditionally, viral decay dynamics after drug treatment is investigated using models of differential equations in which both the death rate of infected cells and the viral production rate are assumed to be constant. Here, we describe age-structured models of the viral decay dynamics in which viral production rates and death rates depend on the age of the infected cells. In order to investigate the effects of age-dependent rates, we compared these models with earlier descriptions of the viral load decay and fitted them to previously published data. We have found no supporting evidence that infected-cell death rates increase, but cannot reject the possibility that viral production rates increase, with the age of the cells. In particular, we demonstrate that an exponential increase in viral production with infected-cell age is perfectly consistent with the data. Since an exponential increase in virus production can compensate for the exponential loss of infected cells, the death rates of HIV-1-infected cells may be higher than previously anticipated. We discuss the implications of these findings for the life span of infected cells, the viral generation time, and the basic reproductive number, R_0 .

An important step in the understanding of the replication dynamics of human immunodeficiency virus type 1 (HIV-1) was made in 1995 when Ho et al. (10) and Wei et al. (26) found that concentrations of HIV-1 in plasma drop rapidly after the administration of antiretroviral drugs. The fast exponential decline was associated with the rapid loss of virus-producing cells, which suggested high turnover of HIV-1-infected cells. Later, the acquisition of more data points charting the decrease in concentrations of HIV-1 in plasma during the first week of treatment indicated a shoulder phase during the first day after treatment, which was explained by the decay of viral particles that had been released already at the start of treatment and therefore were not affected by the administered protease inhibitor (19). In 1999, however, Ramratnam et al. (20) measured a very short half-life of viral particles, and the shoulder phase is now typically explained by the intracellular delay of virus production (8). The consensus view now is that the viral generation time consists of an intracellular delay of around 24 h and a lifetime of virus-producing cells of about 1 day, adding up to roughly 2 days (2).

Traditionally, virus dynamics is investigated using models of ordinary differential equations in which both the death rate of infected cells and the viral production rate are assumed to be constant (17, 18). In contrast to those assumptions, it is biologically plausible that the rate of virus production is initially

low and increases with the age of the infected cell, where age is defined as the time that has passed since the infection of the cell. Further, assuming a constant likelihood that a cell will die (i.e., a constant death rate) results in exponentially distributed life spans of infected cells. However, it is known that life spans of cells need not necessarily be exponentially distributed (3), and previous studies have shown that assuming nonexponential life spans for infected cells can cause problems in estimating parameters of the viral life cycle (13, 15). The true dependence of infected-cell death rates and viral production rates as functions of the age of cells is unknown to date (9). Recently, Reilly et al. (23) attempted to determine the total virus production by simian immunodeficiency virus-infected CD4⁺ T cells in rhesus macaques and found supporting evidence for an exponential increase in the rate of virus production with the age of the infected cell. This behavior has already been indicated in a prior study with visna virus (7). In general, it is of great interest to know the kinetic profile of the viral production rate and the age dependency of infected-cell death rates in order to understand how much virus an infected cell produces and how long the cell lives in vivo.

Age-structured models of virus dynamics based on partial differential equations have received attention recently (5, 11, 14, 24). In these systems, classes of infected cells are structured according to the time that has passed since the cells were infected with a viral particle. Each class of cells has a certain age, with corresponding age-dependent death and viral production rates (Fig. 1). In this study, we have derived a general framework for an age-structured model of virus dynamics after drug treatment. We apply the model to previously published data on HIV-1 decay (19) in order to investigate the effects of different kinetic profiles of viral production rates and age-dependent infected-cell death rates. Generally, we have

* Corresponding author. Present address: Institute of Social and Preventive Medicine (ISPM), University of Bern, 3012 Bern, Switzerland. Phone: 41 31 631 35 29. Fax: 41 31 631 35 20. E-mail: christian.althaus@alumni.ethz.ch.

† Supplemental material for this article may be found at <http://jvi.asm.org/>.

[∇] Published ahead of print on 20 May 2009.

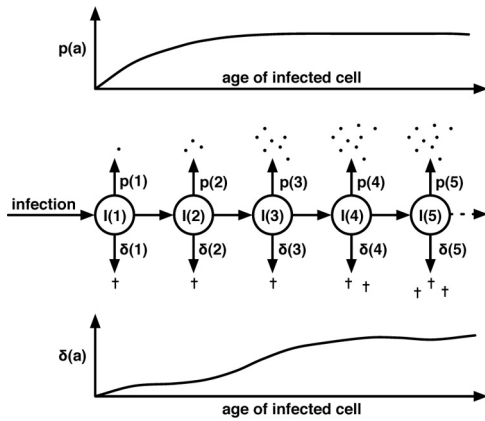


FIG. 1. Illustration of an age-structured model of virus dynamics. After the event of infection, an infected cell moves through different classes of cell populations $I(a)$ that are structured according to the time that has passed since infection. Each of these classes has a corresponding age-dependent viral production rate $p(a)$ (top) and infected-cell death rate $\delta(a)$ (bottom) that can be defined arbitrarily. Black dots and crosses indicate the corresponding amounts of generated virus particles and cell death, respectively.

found no evidence in these data that infected-cell death rates increase, but cannot reject the possibility that viral production rates increase, with the age of infected cells. Interestingly, the exponential increase in the viral production rate indicated by Haase et al. (7) and Reilly et al. (23) is perfectly consistent with these data and would mask the death rates estimated from the HIV-1 decay after drug treatment. Our results indicate that the death rates of HIV-1-infected cells may be higher than previously anticipated, and we discuss how the life span of infected cells, the viral generation time, and the basic reproductive number, R_0 , will be affected.

MODEL

We have derived an age-structured model of virus dynamics based on partial differential equations, similar to that in a study by Nelson et al. (14) (Fig. 1):

$$\frac{dT}{dt} = \lambda - \beta TV - \delta_T T \tag{1}$$

$$\frac{\partial I(a, t)}{\partial t} + \frac{\partial I(a, t)}{\partial a} = -\delta(a)I(a, t) \tag{2}$$

Uninfected CD4⁺ target cells, T , are produced at a rate of λ cells per day, die at the rate δ_T , and become infected by viral particles, V , at a rate of β per particle per day. $I(a, t)$ is defined as the density of infected cells, I , at time t and of age a that die with an age-dependent death rate of $\delta(a)$ per day. New viral particles are produced according to the following equation:

$$\frac{dV}{dt} = \int_0^\infty p(a)I(a, t)da - cV \tag{3}$$

with $p(a)$ being the viral production kernel (i.e., the age-dependent viral production rate) and c being the rate of clearance of free viral particles. The boundary condition for the

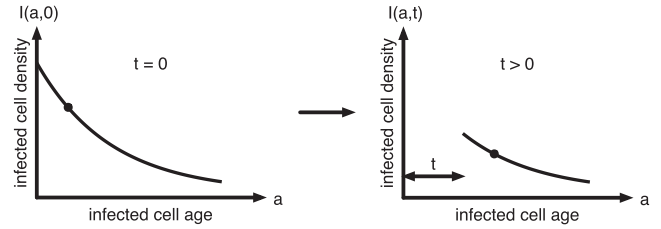


FIG. 2. Density of infected cells, $I(a, t)$, as a function of infected-cell age, a , and the time, t , after drug treatment. At the start of treatment ($t = 0$), the infected cells will be in an equilibrium distribution that, assuming a constant death rate, declines exponentially with the age of the infected cell. During treatment ($t > 0$), de novo infections have stopped and the ages of all infected cells can be defined as $a \geq t$. Thus, the density of infected cells that had a specific age at the start of treatment (black dot) will further decrease during treatment and shift along the axis of infected-cell age.

infected cells, $I(a, t)$, is given simply as the infection of target cells, T , as follows:

$$I(0, t) = \beta VT \tag{4}$$

As viral decay is a fast process (20), we can set the virus into a quasi-steady state (1).

$$V(t) = \frac{1}{c} \int_0^\infty p(a)I(a, t)da \tag{5}$$

Drug treatment. The rationale of antiretroviral drug treatment is to stop new infections by reducing β substantially. Protease inhibitors render the newly produced viral particles noninfectious so that the viral production rate is not affected but β is reduced. Viral particles that are already released from a virus-producing cell at the start of treatment will be unaffected by the protease inhibitor and cause de novo infections of cells during drug treatment. However, since the free viral particles are cleared very rapidly, at a rate of approximately 23 per day (20), we make the assumption that the influence of de novo infections becomes negligible. In the appendix, we derive and discuss a full model that includes the viral particles that are unaffected by the protease inhibitors. For the matter of simplicity, we assume 100% drug efficacy and therefore set β at 0 after the start treatment. The boundary condition in equation 4 will change to $I(0, t) = 0$, except at the start of treatment, where it is given as $I(0, 0) = \beta V(0)T(0)$. Since we make the assumption that de novo infections have stopped, at any point in time during treatment, t , all infected cells have an age of $a \geq t$ and the density of the cells is given as follows:

$$I(a, t) = I(a - t, 0)e^{-\int_a^{a-t} \delta(s)ds} \quad \text{for } a \geq t \tag{6}$$

where s denotes the integration variable for the age-dependent death rate. We further define $I(a, 0)$ as the equilibrium distribution of infected cells with age a at time zero, i.e., at the beginning of treatment (Fig. 2):

$$I(a, 0) = I(0, 0)e^{-\int_0^a \delta(s)ds} \tag{7}$$

Then,

TABLE 1. Age-structured models describing HIV-1 decay after drug treatment^a

Model	Viral production [$p(a)$ for $a \geq \tau$]	Infected-cell death [$\delta(a)$ for $a \geq \tau$]	Viral load [$V(t)$ for $t \geq \tau$]
1	Constant: p_0	Constant: δ_0	$V(t) = V(\tau)e^{-\delta_0(t - \tau)}$
2	Linear: $x(a - \tau)$	Constant: δ_0	$V(t) = V(\tau)[1 + \delta_0(t - \tau)]e^{-\delta_0(t - \tau)}$
3a	Exponential: $p_0e^{x(a - \tau)}$	Constant: δ_0	$V(t) = V(\tau)e^{-(\delta_0 - x)(t - \tau)}$
3b	Exponential: $e^{ax} - 1$	Constant: δ_0	$V(t) = \frac{V(\tau)}{x}[(x - \delta_0)e^{-\delta_0 t} + \delta_0 e^{-(\delta_0 - x)t}]$
4	Sigmoidal: $p_0\left(1 - e^{-\frac{a^2}{x}}\right)$	Constant: δ_0	$V(t) = \frac{p_0 I(0, 0)}{c} \int_t^\infty \left(1 - e^{-\frac{a^2}{x}}\right) e^{-\delta_0 a} da$
5	Models 1 to 4	Linear: $\delta_0[1 + y(a - \tau)]$	Equation 11
6	Models 1 to 4	Exponential: $\delta_0 e^{y(a - \tau)}$	Equation 11

^a Infected cells produce virus after an intracellular delay, τ , according to their viral production kernels, i.e., $p(a) = 0$ for $a < \tau$. The age-dependent death rate, $\delta(a)$, can increase after the infected cells start to produce virus. Since the death rate of infected cells before the productive stage cannot be estimated, the following applies: $\delta(a) = \delta'$ for $a < \tau$, where δ' can have any arbitrary value. Models 1 to 4 have different viral production kernels, while the infected-cell death rate is constant. Models 5 and 6 incorporate linearly and exponentially increasing death rates, respectively, in combination with different viral production kernels. For models 1 to 3b, an explicit solution for the viral load decay is given, while models 4 to 6 can be described only in integral form. During the intracellular delay, the viral load is constant and given as follows: $V(\tau) = V(0)$.

$$I(a - t, 0) = I(0, 0)e^{-\int_0^{a-t} \delta(s) ds} \tag{8}$$

and substituting $I(a - t, 0)$ into equation 6 gives

$$I(a, t) = I(0, 0)e^{-\int_0^{a-t} \delta(s) ds} e^{-\int_a^\infty \delta(s) ds} \tag{9}$$

which simplifies into

$$I(a, t) = I(0, 0)e^{-\int_0^a \delta(s) ds} \tag{10}$$

By substituting $I(a, t)$ into equation 5 and integrating from time t to ∞ , we can account for the total viral production during drug treatment:

$$V(t) = \frac{I(0, 0)}{c} \int_t^\infty p(a)e^{-\int_0^a \delta(s) ds} da \tag{11}$$

with $I(0, 0)$ being the density of infected cells of age 0 at the start of treatment, i.e., the boundary condition as given in equation 4.

Using different types of infected-cell death rates, $\delta(a)$, and viral production kernels, $p(a)$, equation 11 gives us a description of the viral load decay after the start of drug treatment. We therefore fitted several models to previously published data on HIV-1 load decay (19). The data consist of HIV-1 RNA concentrations in plasma samples from five infected patients that were given a protease inhibitor (ritonavir) orally. We time-shifted the data to account for the pharmacokinetic delay as given by Perelson et al. (19) and possibly allow for an additional intracellular delay, τ , corresponding to the viral eclipse phase. The model was fitted to the log-transformed data in Mathematica (version 6.0.1) by using the FindMinimum routine to minimize the sum of squared residuals (SSR).

RESULTS

In order to investigate the effects of age-dependent viral production and infected-cell death rates, we compared age-structured models to a standard model of HIV-1 decay after drug treatment. This allowed us to build up complexity in the description of virus dynamics and test the hypotheses that viral

production rates and infected-cell death rates are increasing with the age of infected cells. The mathematical equations underlying each model are provided in Table 1 and are graphically depicted in Fig. 3 (see also Fig. A1A). First, we evaluate the influence of different viral production kernels.

In the standard model, the viral production kernel and the infected-cell death rate are kept constant and do not depend on infected-cell age (Table 1, model 1). After an intracellular delay, τ , the virus dynamics follows a simple exponential decay pattern with rate δ_0 , i.e., the decay is equal to the loss of infected cells (Fig. 3A).

As a first extension of the model, we assume that the viral production rate is increasing linearly with the age of the infected cell (Table 1, model 2). Interestingly, the slope of the linear increase in viral production, x , does not influence the slope of the viral load decay. The model fits the data well (Fig. 3C) but shows different properties from model 1. The estimated intracellular delay is much shorter (Table 2 and Fig. 3D), the graph of the decline in the viral load is curved, and the decay eventually reaches an exponential decline with slope δ_0 . Hence, because exponential decay is approached only later during treatment, the estimated death rates are higher than those in the standard model (Table 2).

Second, we test the hypothesis of an exponentially increasing viral production rate (Table 1, models 3a and 3b). Surprisingly, model 3a results in exactly the same fit as the standard model, since an exponential increase in viral production compensates for the exponential loss of infected cells (Table 1; Fig. 3A and B). The decline slope is now given as the difference between the death rate and the exponential increase in the production rate, $\delta_0 - x$, which makes it impossible to identify δ_0 or x alone. In model 3b, we change the function for an exponentially increasing production rate so that it starts at zero to account for an intracellular delay (Fig. 3F). This results in biexponential decline (Table 1 and Fig. 3E) that eventually approaches the same rate given in model 3a. However, with model 3b, we estimate infected-cell death rates that are almost three times higher than those in the standard model (Table 2).

In the standard model, virus production starts immediately

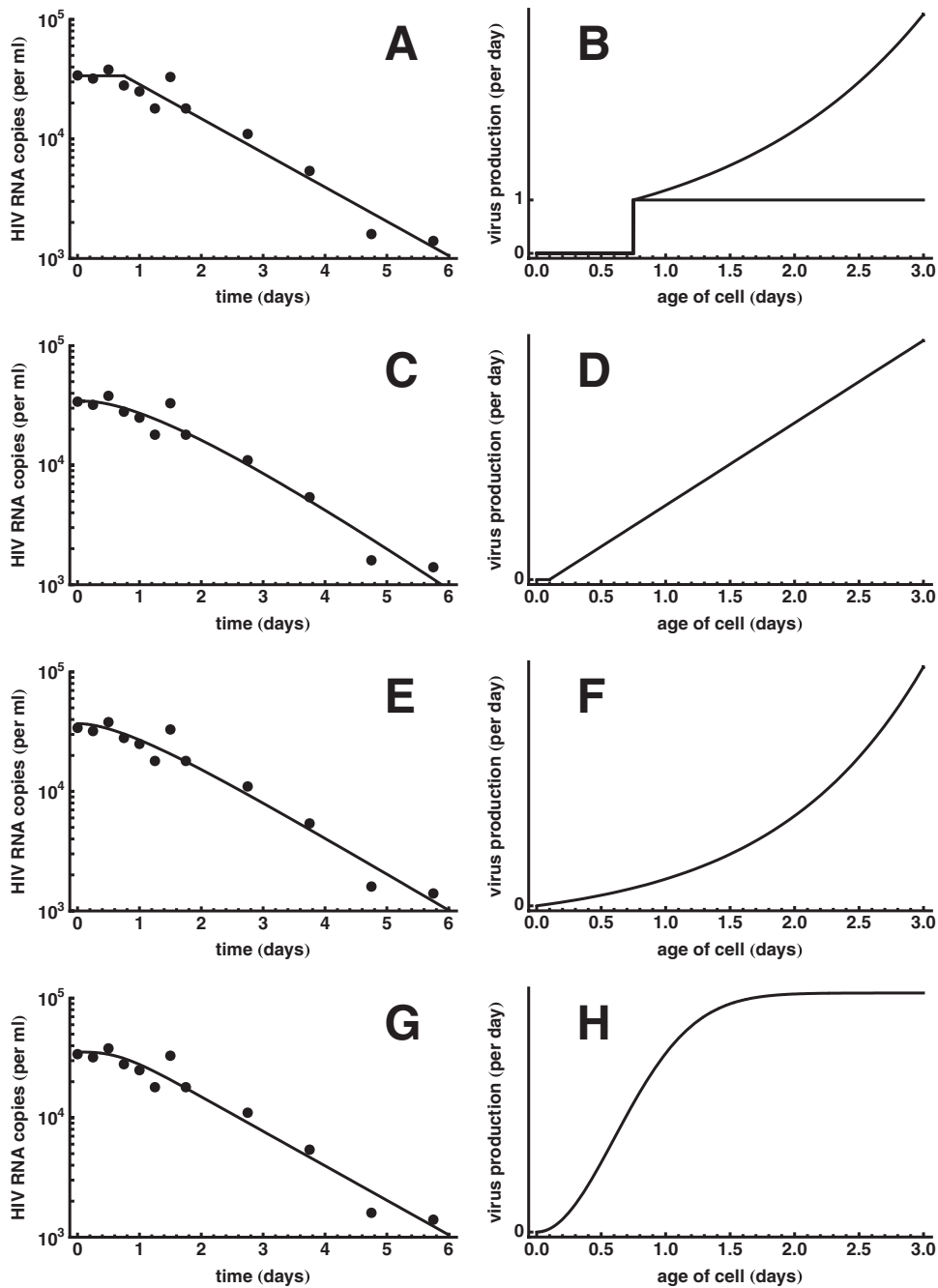


FIG. 3. HIV-1 decay after drug treatment. The results of fitting four different models (solid lines) to data on HIV-1 RNA concentrations (dots) reported by Perelson et al. (19) are depicted in the panels on the left. For each model, the corresponding viral production kernel, $p(a)$, is shown in the panel on the right. Typically, viral production starts after the intracellular delay, τ . (A and B) A constant production rate and an exponentially increasing production rate yield the same decay dynamics; (C and D) linearly increasing production; (E and F) exponentially increasing production starting at zero; (G and H) sigmoidally increasing production. Table 1 gives the mathematical descriptions of the models. Estimated parameters are given in Table 2. The left panels show the results of fitting the models to the data for patient 103, whereas additional patient data with the corresponding fittings are provided in the supplemental material.

at a constant rate after the intracellular delay. To describe the transition to virus production more realistically, we use a sigmoidally increasing virus production rate that is reaching a constant (Table 1, model 4; Fig. 3H). Not surprisingly, the fits look very similar to those for the standard model, with the

exception of a smooth transition from the shoulder phase to the exponential decay of the viral load (Fig. 3G).

It is tempting to speculate about whether increases in viral production rates with the age of infected cells are mechanistically linked to increases in infected-cell death rates with the

TABLE 2. Estimated parameter values from models 1 to 4 for data from five patients in a previous study^a

Patient	Parameter	Value from model:				
		1	2	3a	3b	4
102	δ_0 (day ⁻¹)	0.27	0.47		1.14	0.26
103	δ_0 (day ⁻¹)	0.66	0.93		1.55	0.67
104	δ_0 (day ⁻¹)	0.48	0.70		1.36	0.48
105	δ_0 (day ⁻¹)	0.49	0.72		1.37	0.49
107	δ_0 (day ⁻¹)	0.49	0.72		1.37	0.49
	Mean of δ_0 (day ⁻¹)	0.48	0.71		1.36	0.48
	σ of δ_0 (day ⁻¹)	0.14	0.16		0.15	0.15
	τ (h)	18	2	18		
	x				0.86 day ⁻¹	20 h
	Average life span (days)	3.03	1.56		0.75	2.30
	Generation time (days)	3.03	3.05	3.03	2.93	2.97
	R_0	13.6	11.4		8.7	10.1
	SSR	0.55	0.59	0.55	0.57	0.56

^a Models 1 to 4, summarized in Table 1, were fitted to the data from five patients in a study by Perelson et al. (19). The means and standard deviations of the death rates of infected cells are given, together with the average life spans, the mean generation times, and the basic reproductive numbers (R_0). For model 3a, only the difference between the death rate and the exponential increase in viral production can be estimated, which makes it impossible to calculate the life span. Models 1 to 3a have an intracellular delay, τ , whereas model 3b and model 4 contain the parameter x , defining the increase in the viral production rate (Table 1). The models differ only slightly in their SSR, with the standard model (model 1) together with model 3a yielding the lowest SSR. For the sigmoidally increasing production (model 4), the half-maximal viral production rate is reached at 17 h after infection.

age of cells. The release of HIV-1 particles from the cell may cause disruption of the cell membrane, which may increase the likelihood of cell death and therefore increase the rate at which infected cells die with increasing age. Thus, we also investigated the possibility of age-dependent infected-cell death rates that are either linearly (Table 1, model 5) or exponentially (i.e., following the Gompertz law [6]) (Table 1, model 6) increasing with the age of the cell. We combined these models with the different viral production kernels from models 1 to 4. Generally, increasing infected-cell death rates with the age of infected cells results in decay dynamics characterized by a slope increasing with ongoing treatment (see Fig. A1C). Since the viral load decay data usually approximate an exponential slope after a few days, the fittings resulted in minuscule values for the relative increase in the infected-cell death rates, γ , indicating that a constant death rate for infected cells describes the viral load decay best.

To analyze the results from applying different viral production kernels to the viral load decay data, we can compare the quality of the fittings of the different models. The numbers of parameters for all our models are equal. Each of the five patients is described with a particular infected-cell death rate (i.e., giving five different δ_0 values) and an individual viral load at the start of treatment [i.e., giving five different $V(0)$ values]. Depending on the model, there is an additional parameter for the intracellular delay (τ) or one that describes the increase of the viral production rate (x). Both τ and x are forced to be the same for all five patients. Hence, we have 11 parameters in total and simply compare the SSR among our models (Table 2). Because the standard model fits the data well, we do not find supporting evidence for an increase in viral production rates with the age of the cell. Still, the SSR for the models with different viral production kernels are very similar, which indicates that all models describe the data well with equal numbers of parameters. This observation is interesting, as we cannot reject the hypothesis of increasing viral production rates. We find that models with increasing viral production rates can result in markedly higher estimates of the infected-cell death

rates (Table 2). Further, we have found a special case of an exponentially increasing viral production rate (Table 1, model 3a) that cannot be determined from viral load decay data because it may be hidden in the exponential slope of the viral load decay. This finding also indicates that the death rates of HIV-1-infected cells may be higher than anticipated by fitting the standard model to the viral load decay data.

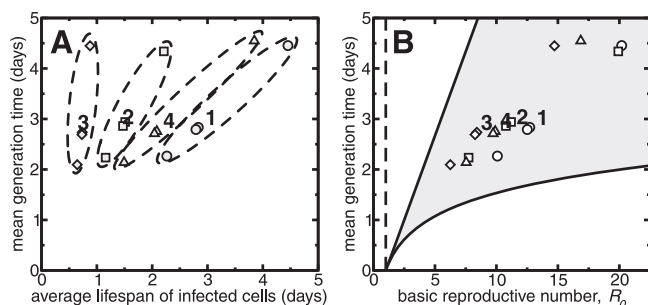


FIG. 4. Life spans of infected cells, viral generation times, and the basic reproductive number, R_0 . (A) Data for each patient are plotted with the estimated average life spans of infected cells and the mean viral generation times. The basic model (model 1; circles) with a constant viral production rate results in the lowest estimates for the death rate of infected cells and therefore yields the longest life span of infected cells. The models with viral production rates that are either linearly (model 2; squares), exponentially (model 3b; diamonds), or sigmoidally (model 4; triangles) increasing result in shorter life spans of infected cells. In contrast, the viral generation time is hardly affected by the different models. Each set of symbols indicating values derived from a certain model for individual patients is surrounded by a dashed ellipse. (B) Models in which viral production rates increase with the age of the infected cell result in smaller basic reproductive numbers. The gray area depicts the range of basic reproductive numbers given a certain viral generation time that can be either fixed or exponentially distributed (25). The dashed line indicates the threshold of R_0 of 1. In both panels, the data for individual patients are indicated by symbols. The locations of the bold numbers corresponding to the models represent the means for all patients in the indicated models. Note that data for patient 105 and patient 107 overlap since the estimated parameters for these patients are equal.

Given the possibility that viral production rates increase with the age of infected cells, we investigated how increasing viral production rates affect the dynamics of the virus replication and the viral turnover. Therefore, we calculated how higher estimates of the infected-cell death rate affect the average life span of infected cells and the viral generation time (see the appendix for the mathematical definitions). Not surprisingly, models with increasing viral production rates result in much shorter average life spans for the infected cells (Fig. 4A). In contrast, the viral generation time is hardly affected by the different models. Since the models resulting in higher estimates for the infected-cell death rate have a viral production rate that is increasing with the age of the infected cell, the majority of viral particles are produced late during the viral life cycle, which compensates for the shorter life spans of infected cells. Another interesting property of virus replication is the basic reproductive number, R_0 (see the appendix for the mathematical definitions). Due to different underlying distributions of the generation time among the different models (see Fig. A2), we find that our estimates for R_0 are generally smaller than the one derived from the standard model (Fig. 4B).

We can conclude that constant viral production and infected-cell death rates are appropriate assumptions to describe HIV-1 dynamics, but we predict that infected-cell death rates tend to be higher if viral production rates increase with the age of infected cells. If that is the case, the life span of the infected cell tends to be shorter and the basic reproductive number decreases whereas the mean viral generation time is unaffected by the assumption that viral production rates increase with the age of the infected cell.

DISCUSSION

In this study, we have derived a general framework for age-structured virus dynamics after drug treatment. Our aim was to investigate the effects of age-dependent viral production rates and infected-cell death rates among HIV-1-infected cells. By fitting different models to previously published data from Perelson et al. (19), we tested the hypotheses of age-dependent viral production rates and infected-cell death rates. We find no evidence for the increase of cell death rates with the ages of the infected cells. It is important to highlight that, due to the restrictions from viral load decay data, we are able to infer the behavior of infected cells only during the first 7 days after infection. Additionally, we are unable to investigate the death of infected cells during the intracellular delay, since the removal of infected cells before they start to produce viral particles will not affect the dynamics of virus production. It is possible that the infected-cell death rate is low initially, during the intracellular delay, but increases during the transition of the cell into the productive stage and saturates at a constant value. However, since an increase in the infected-cell death rate always results in an increasing slope for the viral load decay (see the appendix), the increase in the infected-cell death rate would occur very rapidly after the intracellular delay. Since such behavior is hardly detectable from the viral load decay data, we can summarize that a constant rate of death of infected cells describes the viral load decay dynamics best. Still, the result is surprising, as *in vitro* studies have shown that HIV-1 infection has cytopathic effects. For a summary of those

studies, we refer to Funk et al. (4). Cytopathicity would likely result in an age-dependent increase of the infected-cell death rate. However, the situation *in vivo*, where the majority of infected-cell death is imposed by cytotoxic-T-lymphocyte-mediated killing, is likely to be different. In the case in which cytotoxic T lymphocytes have to search for infected target cells to deliver their lethal hit, a constant rate of death and, therefore, exponentially distributed life spans of the cells may serve as appropriate descriptions of the virus dynamics (22).

In contrast to the hypothesis of increasing infected-cell death rates, the possibility that viral production rates increase with the age of the infected cell cannot be rejected. We have found that different models with increasing viral production rates describe the viral load decay data well and that they can result in markedly higher estimates of infected-cell death rates. Since the true dependence of the kinetic profile of viral production is unknown, we can only speculate whether our different models with increasing viral production rates are adequate to describe the virus dynamics. For example, given the biology underlying the intracellular kinetics of HIV-1 replication (21), it is questionable whether model 2 ($\tau = 2$ h) and model 3b (no intracellular delay at all) describe the virus production realistically. The mathematical models we present here try to capture a specific feature of the kinetic profile of virus production, such as the strength of the increase with the age of the cell or the smooth transition from the intracellular delay into the phase of virus production. Biological reality may be somewhere in between those models, but since we generally find higher estimates for the infected-cell death rates with viral production rates increasing with the age of the cell, we highlight that the death rates of HIV-1-infected cells may be higher than previously anticipated. This possibility would in turn imply shorter average life spans of infected cells. Due to a different kinetic profile of virus production, we have also found that these models result in smaller values for the basic reproductive number. However, the mean viral generation time, i.e., the average time it takes from the infection of a cell until a viral particle from that cell will infect a new cell, is not affected by the different models. Hence, the turnover rate of HIV-1 within a patient does not depend on the kinetic profile of virus production.

Perhaps more interesting, we also found a special case with an exponential increase in the viral production rate that cannot be ruled out by viral load decay data because it provides an identical fit (Fig. 3A). It has been suggested recently that viral production increases exponentially in simian immunodeficiency virus-infected cells from rhesus macaques. Reilly et al. (23) estimate an exponential increase in viral production, with an exponent of 0.1 day^{-1} , for activated CD4^+ T cells. This finding is also supported by the results of a study of visna virus that suggest an exponential increase in viral production that levels off after a few days (7). Because we cannot exclude the possibility that the viral production is indeed increasing exponentially, the observed exponential slope of viral load decay would represent the difference between infected-cell death and the exponential increase in virus production. If the estimate from Reilly et al. (23) was realistic, we would have to increase the previous estimates of HIV-1-infected-cell death rates by 0.1 day^{-1} . In addition, the assumption of 100% drug efficacy also implies that the estimates of the infected-cell death rates

always have to be taken as minimal estimates (19). Together, these two factors would result in much shorter life spans of HIV-1-infected cells than previously thought. However, it remains to be ascertained whether exponentially increasing viral production rates also occur for HIV-1 in vivo and, if there was a leveling off, at what time it would take place.

Further analyses of the dynamics of virus production will be required to decipher the true kinetic profile of virus production. As there are limitations in measuring HIV-1-infected cells and virus production in a patient in greater detail, it is most likely that further in vitro studies under conditions that are close to an in vivo situation are required to shed new light on the issue.

ACKNOWLEDGMENTS

We thank Alan Perelson for kindly providing us the viral load data, Libin Rong for discussions about the derivation of the age-structured model, Vitaly Ganusov for providing a Mathematica notebook to fit multiple data sets, and Jacco Wallinga, Henk-Jan van den Ham, Tendai Mugwagwa, and Boris Schmid for critically reading the manuscript. We also thank two anonymous reviewers for helpful comments.

C.L.A. and R.J.D.B. gratefully acknowledge financial support by The Netherlands Organization for Scientific Research (VICI grant 016.048.603).

APPENDIX

The special case of protease inhibitors. In the text, we made the assumption that the administration of antiretroviral drugs reduces the infection rate, β . While this is true for reverse transcriptase inhibitors, protease inhibitors render newly produced viral particles noninfectious. Thus, the viral particles that have already been released from the virus-producing cells at the start of therapy will be unaffected by the protease inhibitor. We extend our model to include a population of infectious viral particles that cause de novo infections of cells during drug treatment.

The free viral particles at the start of treatment are represented simply by $V(0)$. Since they are unaffected by the protease inhibitor and still infectious, we use the term $V_i(0)$. Following therapy, they disappear at clearance rate c , i.e., $V_i(t) = V_i(0)e^{-ct} = V(0)e^{-ct}$. Therefore, the boundary condition from equation 4 will not be zero but decreases according to the following: $I(0, t) = \beta V(0)T(0)e^{-ct} = I(0, 0)e^{-ct}$, where we have to assume that the number of target cells, T , stays constant during the very early period of drug treatment. Now, we describe the density of infected cells that have been produced de novo during treatment, i.e., the infected cells with age $a < t$:

$$I(a, t) = I(0, t - a)e^{-\int_0^a \delta(s) ds} \quad \text{for } a < t \quad (12)$$

Substituting the time-dependent boundary condition, $I(0, t)$, into equation 12 gives

$$I(a, t) = I(0, 0)e^{-c(t-a)}e^{-\int_0^a \delta(s) ds} \quad (13)$$

By substituting $I(a, t)$ into equation 5 and integrating from time zero to t , we can account for the viral particles produced by cells being infected during treatment:

$$V(t) = \frac{I(0, 0)}{c} \int_0^t e^{-c(t-a)} p(a) e^{-\int_0^a \delta(s) ds} da \quad (14)$$

Using equation 14 together with equation 11, we can now describe the total viral production during drug treatment:

$$V(t) = \frac{I(0, 0)}{c} \left(\int_0^t e^{-c(t-a)} p(a) e^{-\int_0^a \delta(s) ds} da + \int_t^\infty p(a) e^{-\int_0^a \delta(s) ds} da \right) \quad (15)$$

We also fitted the full model from equation 5 to the data on HIV-1

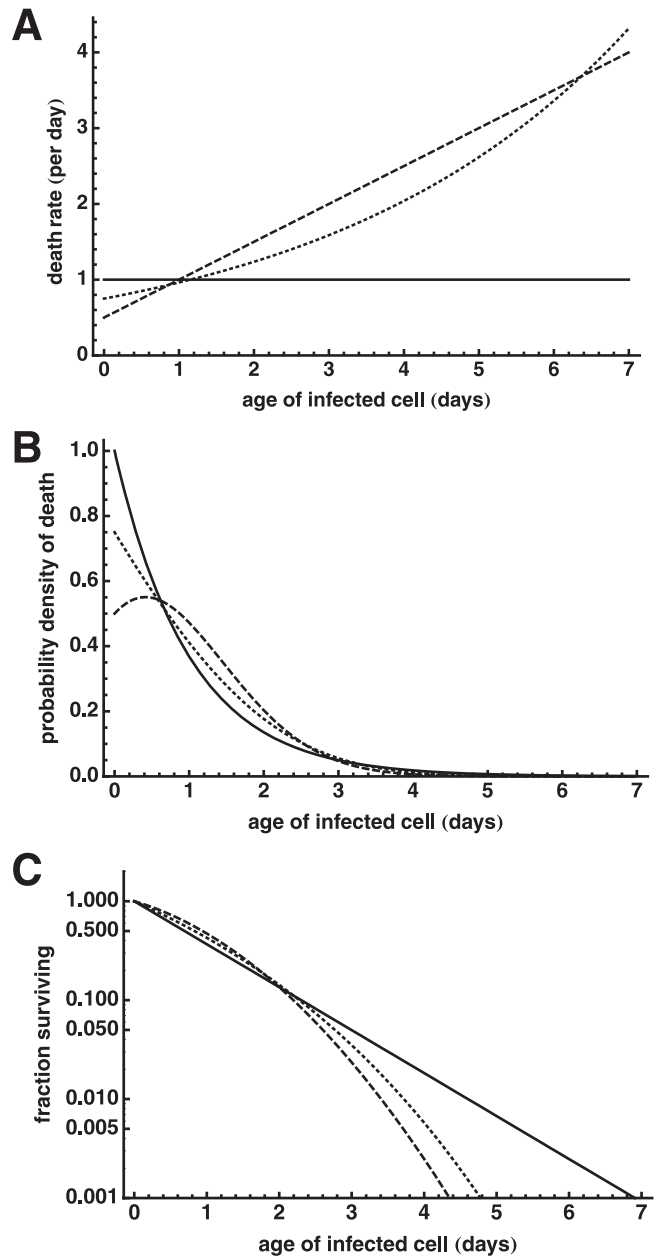


FIG. A1. Relationship among the death rate, the probability density of death, and the fraction of cells surviving as a function of infected-cell age. (A) Infected-cell death rates can either be constant (solid line) or increase linearly (dashed line) or exponentially (dotted line) with the age of the infected cells. (B) These patterns lead to characteristic probability density functions of infected-cell death that are equal to the life span distributions of infected cells. Note that if death rates increase with the age of the infected cell, the life span distributions can become humped. (C) Fractions of infected cells surviving until a certain age. The increase of infected-cell death rates with the age of the cell leads to a decline in the number of infected cells, with an increasing slope (dashed and dotted lines).

load decay. Since viral particles are cleared very rapidly, at a rate of approximately 23 per day (20), the influence of new infections caused by viral particles that are not affected by the protease inhibitor is negligible and does not change our results and parameter estimates.

Infected-cell death rates, probability densities, and survival. Here,

we want to illustrate the relationship among age-dependent death rates for infected cells, the probability density of infected-cell death, and the survival of infected cells. If a population of infected cells experiences an age-dependent death rate, $\delta(a)$ (Fig. A1A), we can derive the survival function for infected cells, i.e., the fraction of cells surviving until age a (Fig. A1C):

$$f(a) = e^{-\int_0^a \delta(s) ds} \quad (16)$$

The age-dependent probability density function of infected-cell death, which is equal to the life span distribution of infected cells, can then be given by the product of the probability that they die at age a [given by $\delta(a)$] and the survival of infected cells (Fig. A1B):

$$\hat{\delta}(a) = \delta(a)e^{-\int_0^a \delta(s) ds} \quad (17)$$

Figure A1C illustrates that if the death rate of infected cells increases with the age of the cells, the fraction of infected cells decreases with an increasing slope (dashed and dotted lines). Therefore, models in which death rates increase with the age of the infected cells cannot easily describe the observed HIV-1 load decay, which typically approaches an exponential decline. Further, the increase in viral production rates with the age of infected cells cannot compensate for the more than exponential loss of infected cells.

Life span and generation time. Our finding that infected-cell death rates may be higher than previously estimated suggests shorter life spans for infected cells. The life span of an infected cell can be defined as the sum of the intracellular delay, τ , and the average life span of a cell in the phase of virus production. With $\hat{\delta}(a)$ being the life span distribution (see equation 17), the average life span, \bar{l} , of an infected cell can be written as

$$\bar{l} = \tau + \int_{\tau}^{\infty} a \hat{\delta}(a) da \quad (18)$$

For the case in which infected-cell death rates are independent of the age of the cell, the life span, \bar{l} , is given simply as $\tau + 1/\delta_0$, where δ_0 is the death rate of the infected cells.

We also want to investigate how the viral generation time is affected by our results. The viral generation time is given as the time between the onsets of two consecutive productive phases of infected cells. This generation time, \bar{g} , can be written as follows:

$$\bar{g} = \tau + \frac{\int_0^{\infty} a p(a) f(a) da}{\int_0^{\infty} p(a) f(a) da} \quad (19)$$

where $p(a)f(a)$ represents the amount of virus that is produced by cells that have reached age a . Note that for $a < \tau$, $p(a) = 0$. In principle, equation 19 needs to be expanded by the term $1/(\beta T)$ to account for the average time that a single viral particle needs to find a new target cell. Unfortunately, this time can hardly be estimated, but considering the short lifetimes of free viral particles, it is likely to be short. Moreover, this time is independent of age-dependent infected-cell death rates or virus production rates.

Basic reproductive number, R_0 . The basic reproductive number, R_0 , for a viral infection within a host can be defined as the number of newly infected cells produced by one infected cell during its lifetime, assuming that all other cells are susceptible. For the period of rapid viral replication early after HIV-1 infection, it is reasonable to make the assumption of maximal target cell availability, and the growth rate of the virus during this phase, measured from the rise in the level of plasma viremia, has been estimated to be ~ 1.5 per day (12). For the standard model (model 1) with a fixed intracellular delay, τ , and constant viral production and infected-cell death rates, the basic reproductive number can be expressed as follows: $R_0 = e^{r\tau}(1 + r/\delta_0)$, where r is the initial growth rate and δ_0 is the death rate of the infected cells (16). However, for the models that have age-dependent viral production kernels, the underlying distribution of the generation time can deviate from an exponential distribution and therefore differs from that in the standard model (Fig. A2). Generally, the generation time distribution, $g(a)$, for infected cells is defined as follows:

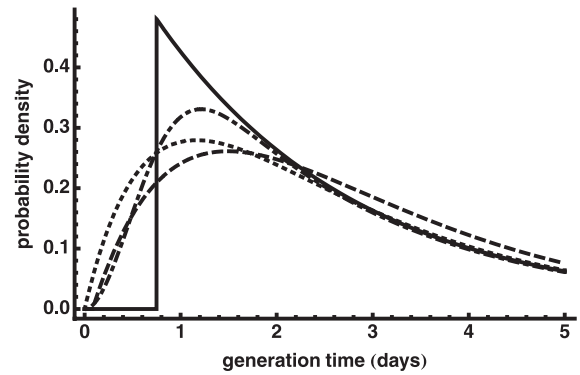


FIG. A2. Generation time distributions resulting from different viral production kernels. Assuming that viral production rates increase with the age of an infected cell influences the shape of the generation time distribution. The standard model (model 1) follows an exponentially distributed generation time after the intracellular delay (solid line). Increases in viral production rates with the age of infected cells result in shorter intracellular delays and a smoothing of the generation time distribution. Dashed line, linearly increasing viral production rate (model 2); dotted line, exponentially increasing viral production rate (model 3a); dashed-dotted line, sigmoidally increasing viral production rate (model 4). Note that the means for all four distributions are roughly the same (Table 2).

$$g(a) = \frac{p(a)f(a)}{\int_0^{\infty} p(a)f(a) da} \quad (20)$$

i.e., it is given by the normalized product of the age-dependent viral production rate, $p(a)$, and the survival probability, $f(a)$, for an infected cell. Wallinga and Lipsitch (25) have recently shown how the distribution of generation times, $g(a)$, shapes the relationship between the growth rate, r , and the basic reproductive number, R_0 , and obtained

$$R_0 = \frac{1}{\int_0^{\infty} e^{-ra} g(a) da} \quad (21)$$

where the denominator can be defined as the Laplace transform of the generation time distribution, $g(a)$. Hence, for the models with viral production rates increasing with the age of the infected cell, we use equation 21 to calculate R_0 .

REFERENCES

1. De Boer, R., and A. Perelson. 1998. Target cell limited and immune control models of HIV infection: a comparison. *J. Theor. Biol.* **190**:201–214.
2. Dixit, N. M., M. Markowitz, D. D. Ho, and A. S. Perelson. 2004. Estimates of intracellular delay and average drug efficacy from viral load data of HIV-infected individuals under antiretroviral therapy. *Antivir. Ther.* **9**:237–246.
3. Dowling, M. R., D. Milutinovic, and P. D. Hodgkin. 2005. Modelling cell lifespan and proliferation: is likelihood to die or to divide independent of age? *J. R. Soc. Interface* **2**:517–526.
4. Funk, G. A., A. Oxenius, M. Fischer, M. Opravil, B. Joos, M. Flepp, R. Weber, H. F. Günthard, and S. Bonhoeffer. 2006. HIV replication elicits little cytopathic effects in vivo: analysis of surrogate markers for virus production, cytotoxic T cell response and infected cell death. *J. Med. Virol.* **78**:1141–1146.
5. Gilchrist, M. A., D. Coombs, and A. S. Perelson. 2004. Optimizing within-host viral fitness: infected cell lifespan and virion production rate. *J. Theor. Biol.* **229**:281–288.
6. Gompertz, B. 1825. On the nature of the function expressive of the law of human mortality, and on a new mode of determining the value of life contingencies. *Philos. Trans. Ser. I* **115**:513–583.
7. Haase, A. T., L. Stowring, J. D. Harris, B. Traynor, P. Ventura, R. Peluso, and M. Brahic. 1982. *Visna* DNA synthesis and the tempo of infection in vitro. *Virology* **119**:399–410.
8. Herz, A. V., S. Bonhoeffer, R. M. Anderson, R. M. May, and M. A. Nowak. 1996. Viral dynamics in vivo: limitations on estimates of intracellular delay and virus decay. *Proc. Natl. Acad. Sci. USA* **93**:7247–7251.
9. Ho, D. D., and Y. Huang. 2002. The HIV-1 vaccine race. *Cell* **110**:135–138.

10. **Ho, D. D., A. U. Neumann, A. S. Perelson, W. Chen, J. M. Leonard, and M. Markowitz.** 1995. Rapid turnover of plasma virions and CD4 lymphocytes in HIV-1 infection. *Nature* **373**:123–126.
11. **Kirschner, D., and G. F. Webb.** 1996. A model for treatment strategy in the chemotherapy of AIDS. *Bull. Math. Biol.* **58**:376–390.
12. **Little, S. J., A. R. McLean, C. A. Spina, D. D. Richman, and D. V. Havlir.** 1999. Viral dynamics of acute HIV-1 infection. *J. Exp. Med.* **190**:841–850.
13. **Lloyd, A. L.** 2001. The dependence of viral parameter estimates on the assumed viral life cycle: limitations of studies of viral load data. *Proc. Biol. Sci.* **268**:847–854.
14. **Nelson, P., M. Gilchrist, D. Coombs, J. Hyman, and A. Perelson.** 2004. An age-structured model of HIV infection that allows for variations in the production rate of viral particles and the death rate of productively infected cells. *Math. Biosci. Eng.* **1**:267–288.
15. **Nelson, P. W., and A. S. Perelson.** 2002. Mathematical analysis of delay differential equation models of HIV-1 infection. *Math. Biosci.* **179**:73–94.
16. **Nowak, M., A. Lloyd, G. Vasquez, T. Wiltrout, L. Wahl, N. Bischofberger, J. Williams, A. Kinter, A. Fauci, V. Hirsch, and J. Lifson.** 1997. Viral dynamics of primary viremia and antiretroviral therapy in simian immunodeficiency virus infection. *J. Virol.* **71**:7518–7525.
17. **Nowak, M., and R. May.** 2000. *Virus dynamics: mathematical principles of immunology and virology.* Oxford University Press, Oxford, United Kingdom.
18. **Perelson, A.** 2002. Modelling viral and immune system dynamics. *Nat. Rev. Immunol.* **2**:28–36.
19. **Perelson, A., A. Neumann, M. Markowitz, J. Leonard, and D. Ho.** 1996. HIV-1 dynamics in vivo: virion clearance rate, infected cell life-span, and viral generation time. *Science* **271**:1582–1586.
20. **Ramratnam, B., S. Bonhoeffer, J. Binley, A. Hurley, L. Zhang, J. Mittler, M. Markowitz, J. Moore, A. Perelson, and D. Ho.** 1999. Rapid production and clearance of HIV-1 and hepatitis C virus assessed by large volume plasma apheresis. *Lancet* **354**:1782–1785.
21. **Reddy, B., and J. Yin.** 1999. Quantitative intracellular kinetics of HIV type 1. *AIDS Res. Hum Retrovir.* **15**:273–283.
22. **Regoes, R., A. Yates, and R. Antia.** 2007. Mathematical models of cytotoxic T-lymphocyte killing. *Immunol. Cell Biol.* **85**:274–279.
23. **Reilly, C., S. Wietgrefe, G. Sedgewick, and A. Haase.** 2007. Determination of simian immunodeficiency virus production by infected activated and resting cells. *AIDS* **21**:163–168.
24. **Rong, L., Z. Feng, and A. S. Perelson.** 2007. Mathematical analysis of age-structured HIV-1 dynamics with combination antiretroviral therapy. *SIAM J. Appl. Math.* **67**:731–756.
25. **Wallinga, J., and M. Lipsitch.** 2007. How generation intervals shape the relationship between growth rates and reproductive numbers. *Proc. Biol. Sci.* **274**:599–604.
26. **Wei, X., S. K. Ghosh, M. E. Taylor, V. A. Johnson, E. A. Emini, P. Deutsch, J. D. Lifson, S. Bonhoeffer, M. A. Nowak, and B. H. Hahn.** 1995. Viral dynamics in human immunodeficiency virus type 1 infection. *Nature* **373**:117–122.